THE JOURNAL OF PHYSICAL CHEMISTRY C

Article

pubs.acs.org/JPCC

Linear Photophysics and Femtosecond Nonlinear Spectroscopy of a Star-Shaped Squaraine Derivative with Efficient Two-Photon Absorption

Taihong Liu,[†] Mykhailo V. Bondar,[*,‡] Kevin D. Belfield,[*,†,§] Dane Anderson,[∥,⊥] Artëm E. Masunov,[∥,⊥,#] David J. Hagan,[#,⊗] and Eric W. Van Stryland[*,#,⊗]

[†]College of Science and Liberal Arts, New Jersey Institute of Technology, University Heights, Newark, New Jersey 07102, United States

[‡]Institute of Physics NASU, Prospect Nauki, 46, Kiev-28 03028, Ukraine

[§]School of Chemistry and Chemical Engineering, Shaanxi Normal University, Xi'an 710062, P.R. China

[∥]NanoScienece Technology Center, University of Central Florida, 12424 Research Parkway, PAV400, Orlando, Florida 32826, United States

[⊥]Department of Chemistry, University of Central Florida, 4111 Libra Drive PSB225, Orlando, Florida 32816-2366, United States

[#]Department of Physics, University of Central Florida, 4111 Libra Drive PSB430, Orlando, Florida 32816, United States

[⊗]CREOL, The College of Optics and Photonics, University of Central Florida, P.O. Box 162366, Orlando, Florida 32816, United States

Supporting Information

ABSTRACT: The synthesis, comprehensive linear photophysical and photochemical study, two-photon absorption (2PA) spectrum, ultrafast relaxation kinetics in the excited states, and efficient superluminescence properties of a new symmetrical three-armed star-shaped squaraine derivative (**1**) are presented. The steady-state spectral parameters of **1** in a number of organic solvents, including fluorescence excitation anisotropy spectra, revealed a weak interaction between the squaraine branches and the effect of symmetry breaking in the ground electronic state. The degenerate 2PA spectrum of **1** was obtained over a broad spectral range with a maximum cross section of ~8000 GM using the open aperture Z-scan technique. The nature of the fast dynamic processes in the excited electronic states of **1** was investigated by the femtosecond transient absorption pump−probe method, revealing characteristic relaxation times of ~3−4 ps. The efficient superluminescence emission of **1** was observed in relatively low concentration solution (≈ $2.3 \cdot 10^{-4}$ M) under femtosecond transverse pumping. A quantum-chemical study of **1** was performed using ZINDO/S//DFTB theory levels. Simulated 1PA and 2PA absorption spectra were found to be in a good agreement with experimental data. The figure of merit for **1** is ~10^{11} GM,[1] one of the highest values ever reported for two-photon fluorescence molecular probes, suggesting strong potential for its application in two-photon fluorescence microscopy and bioimaging.

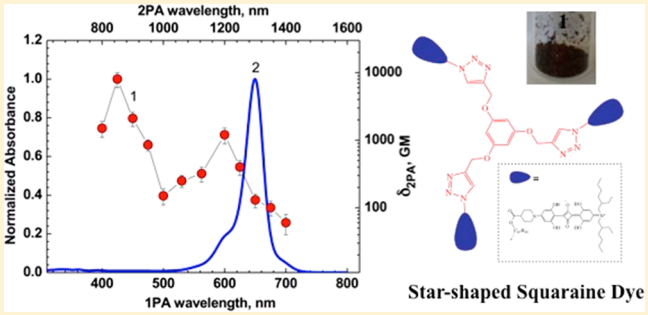

1. INTRODUCTION

Squaraine molecules are a promising class of chromophores with potential applications in a number of scientific and technological areas such as organic electronics,[2−4] optical data storage,[5,6] chemosensing,[7−9] nonlinear optics,[10−12] photodynamic therapy,[13−15] and one- and two-photon fluorescence probes.[16−19] In this regard, the synthesis of new squaraine derivatives and the investigation of their main photophysical, photochemical, and nonlinear optical properties are subjects of intense interest for a variety of optical applications. Squaraines are neutral molecules with a resonance-stabilized zwitterionic structure,[14,20] and typical D-A-D type of electronic distribution,[21,22] where D and A stand for electron-donating terminal groups and electron-deficient (electron acceptor) central oxocyclobutenolate core, respectively. These compounds demonstrate a wide range of linear photophysical and nonlinear optical properties strongly dependent on the nature of the terminal substituents[2,23,24] and molecular symmetry.[25−27]

In particular, the majority of symmetrical squaraines exhibit sharp, intense long wavelength one-photon absorption (1PA) bands,[28,29] high two-photon absorption (2PA) efficiency (maxima cross sections ~$1 \cdot 10^4$ GM),[30,31] high fluorescence

Received: March 8, 2016
Revised: April 15, 2016
Published: May 18, 2016

DOI: 10.1021/acs.jpcc.6b02446
J. Phys. Chem. C 2016, 120, 11099−11110

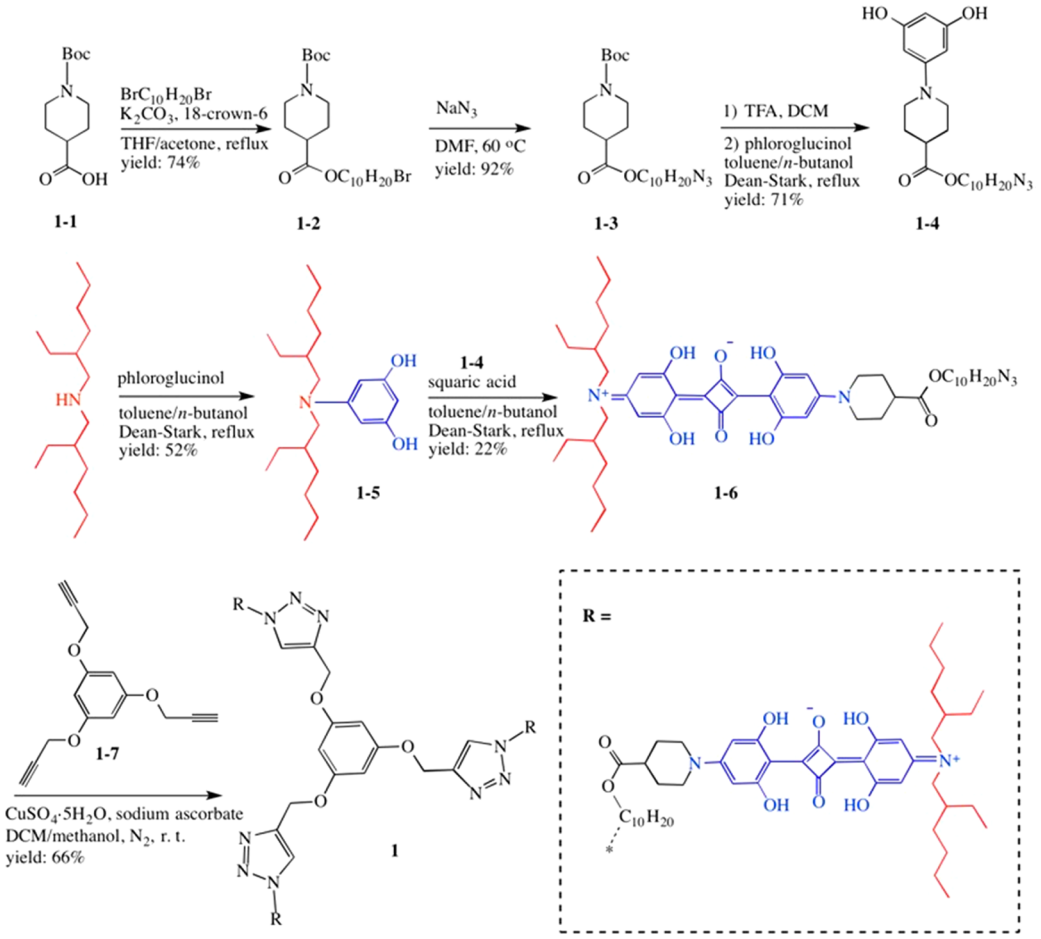

Figure 1. Synthetic route for compound **1**.

quantum yields (~0.4−1.0),[32,33] and high photochemical stability,[11,34,35] that make them promising candidates for two-photon fluorescence microscopy (2PFM) applications, including bioimaging.[18,30] It is worth mentioning that some of the specific nonlinear optical properties such as superluminescence[36,37] (or amplified spontaneous emission) and lasing abilities were recently reported for symmetrical squaraines,[11] and can be employed in the development of a new generation of fluorescent labels with increased brightness and high spectral resolution.[38,39]

Here we report the synthesis and comprehensive characterization of the linear spectroscopic, photochemical, and nonlinear optical properties of a three arm star-shaped squaraine derivative (**1**), including excitation anisotropy, two-photon absorption (2PA), femtosecond pump−probe spectroscopy, superluminescence, and symmetry breaking phenomena. The nature of the electronic characteristics of the molecular structure of **1** was also investigated by quantum-chemical calculations at DFTB[40] and ZINDO/S[41] levels of theory. Linear spectroscopic, photochemical, and nonlinear optical parameters obtained for **1** revealed its potential for application in 2PFM techniques.

2. EXPERIMENTAL SECTION

2.1. Synthesis of Star-Shaped Squaraine 1. Reagents and conditions for the synthesis of **1** are presented in Figure 1. The star-shaped squaraine derivative **1** was accomplished by first synthesizing the azide-containing unsymmetrical squaraine dye (**1-6**) and then coupling this to 1,3,5-tris(2-propynyloxy)-benzene (**1-7**) via click chemistry. Initially, the synthesis of precursors **1-4** and **1-5** are based on the general reactivity of phloroglucinol with secondary amines through its keto tautomer in *n*-butanol/toluene mixture at reflux temperature. Unsymmetrical squaraine **1-6** was synthesized from the condensation of electro-rich aromatic compounds **1-4** and **1-5** with squaric acid using a Dean−Stark apparatus, where the water that formed was removed continuously. The chemical structure and purity of the related compounds were confirmed by ^{1}H and ^{13}C NMR and high-resolution mass spectroscopy. Synthetic and molecular characterization details are presented in the Supporting Information.

2.2. Linear Photophysical and Photochemical Characterization of 1. All linear spectroscopic measurements were carried out at room temperature in spectroscopic grade solvents: toluene (TOL), tetrahydrofuran (THF), dichloromethane (DCM), and acetonitrile (ACN), purchased from commercial suppliers and used without further purification. The steady-state 1PA spectra of **1** were obtained with a Varian CARY-500 spectrophotometer using 10 mm path length quartz cuvettes and dye concentrations, C ~ 10^{-6} M. The steady-state fluorescence emission and excitation anisotropy spectra, along with the fluorescence lifetimes, τ_{fl}, of **1** were measured with a FLS980 spectrofluorimeter (Edinburg Instruments Ltd.) using 10 × 10 × 48 mm spectrofluorometric quartz cuvettes with C ≤ 10^{-7} M.

The fundamental excitation anisotropy spectrum of **1**, $r_0(\lambda)$, was obtained in viscous polytetrahydrofuran (pTHF) at room temperature, where depolarization effects related to molecular rotational motion are negligible (i.e., the molecular rotational

DOI: 10.1021/acs.jpcc.6b02446
J. Phys. Chem. C 2016, 120, 11099−11110

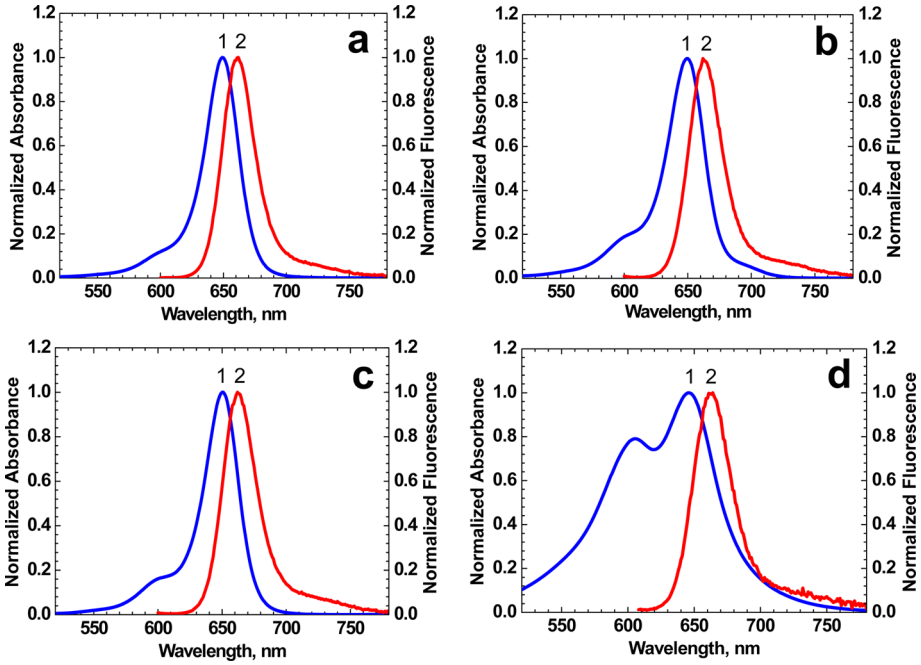

Figure 2. Normalized linear absorption (1) and fluorescence (2) spectra of **1** in TOL (a), THF (b), DCM (c), and ACN (d, excitation wavelength 593 nm).

correlation time, $\theta = \eta \cdot V/kT \gg \tau_{fl}$, where η, V, k, and T are the viscosity of solvent, effective rotational molecular volume, Boltzmann's constant, and absolute temperature, respectively). In this case, the observed experimental value of anisotropy[42]

$$r(\lambda) = \frac{r_0(\lambda)}{(1 + \tau_{fl}/\theta)} \quad (1)$$

is close to $r_0(\lambda)$. The excitation anisotropy spectra of **1**, $r(\lambda)$, were also determined in low viscosity solvents in order to analyze the influence of solvent polarity on the rotational movement of the solute. The values of fluorescence quantum yields of **1**, Φ_{fl}, were obtained by standard methodology[42] relative to Cresyl Violet in methanol as a reference ($\Phi_{fl} \approx 0.54$).[43] The photochemical stability of **1** was investigated quantitatively by measuring the photochemical decomposition quantum yield, $\Phi_{ph} = N_{ph}/N_{hv}$ (N_{ph} and N_{hv} are the numbers of decomposed molecules and absorbed photons, respectively). The values of Φ_{ph} were determined by an absorption method[44] using a continuous wave (CW) diode laser for excitation of **1** into the main absorption band (excitation wavelength, $\lambda_{ex} \approx 650$ nm, average beam irradiance ≈ 30 mW/cm^2). According to well-developed absorption methodology, photodecomposition quantum yields can be determined by the expression:[44]

$$\Phi_{ph} = \frac{[D(\lambda_{ex}, 0) - D(\lambda_{ex}, t_i)] \times N_A}{10^3 \times \varepsilon(\lambda_{ex}) \times \int_\lambda \int_0^{t_i} I_0(\lambda) \times [1 - 10^{-D(\lambda,t)}] \times d\lambda \times dt}$$

where $D(\lambda,0)$, $D(\lambda,t_i)$, N_A, $\varepsilon(\lambda)$, t_i, and λ are the initial and final absorbance of the solution, Avogadro's number, extinction coefficient ($M^{-1}\cdot cm^{-1}$), irradiation time (s), and excitation wavelength (cm), respectively, while $I_0(\lambda)$ is the spectral distribution of the excitation irradiance.

2.3. 2PA Cross Sections, Transient Absorption and Superluminescence Measurements. Nonlinear optical characterization of **1** was performed with a femtosecond laser system, including a Ti:sapphire regenerative amplifier (Legend Duo+, Coherent, Inc.) with output wavelength 800 nm, pulse energy, $E_P \approx 12$ mJ, pulse duration, $\tau_P \approx 40$ fs, and repetition rate 1 kHz, pumped optical parametric amplifier (OPA, HE-TOPAS, Light Conversion, Inc.) with tuning range 1200−2500 nm, and maximum output pulse energy $E_P \approx 1$ mJ. The frequency of the output OPA beam was doubled by a 1 mm BBO crystal and split in two parts for pump and probe laser beams. The first beam was filtered by multiple 10 nm (fwhm) spike filters (output pulse duration, $\tau_P \approx 100$ fs, $E_P \leq 30$ μJ) and used for Z-scan measurements[45] of the degenerate 2PA spectrum of **1** over a broad spectral range. The second beam was focused into a 5 mm sapphire plate to generate a white light continuum (WLC), filtered by the same type spike filters to extract suitable probe wavelengths. Pump and probe laser beams along with the optical delay line were employed in the transient absorption pump−probe setup[11,38] using a 1 mm flow cell for the sample solution to avoid possible photodecomposition and thermooptical effects. The temporal resolution of this pump−probe methodology was estimated to be <240 fs.

The potential for optical amplification of the spontaneous fluorescence emission of **1** was investigated in TOL solution under transverse one-photon pumping by the femtosecond 1 kHz pulse train into the main linear absorption band ($\lambda_{ex} \approx 650$ nm). The second harmonic of the OPA with $\tau_P \approx 100$ fs and $E_P \leq 30$ μJ (see above description) was focused by a cylindrical lens into a spectrofluorometric quartz cuvette (4 × 10 × 38 mm) containing the sample in solution (C $\approx 2.3\cdot10^{-4}$ M) to a waist of 0.15 × 4 mm. The superluminescence emission of **1** was observed in the transverse direction relative to the pump beam and was registered with a fiber optic spectrometer (HR4000, Ocean Optics, Inc.).[11]

2.4. Computational Methodology. To analyze electronic properties of **1**, quantum-chemical calculations were performed with Gaussian 2009, Rev. C1 suite of programs.[46] Due to the large number of atoms, we used DFTB[40] for geometry optimization and ZINDO/S[41] for the description of the

DOI: 10.1021/acs.jpcc.6b02446
J. Phys. Chem. C 2016, 120, 11099−11110

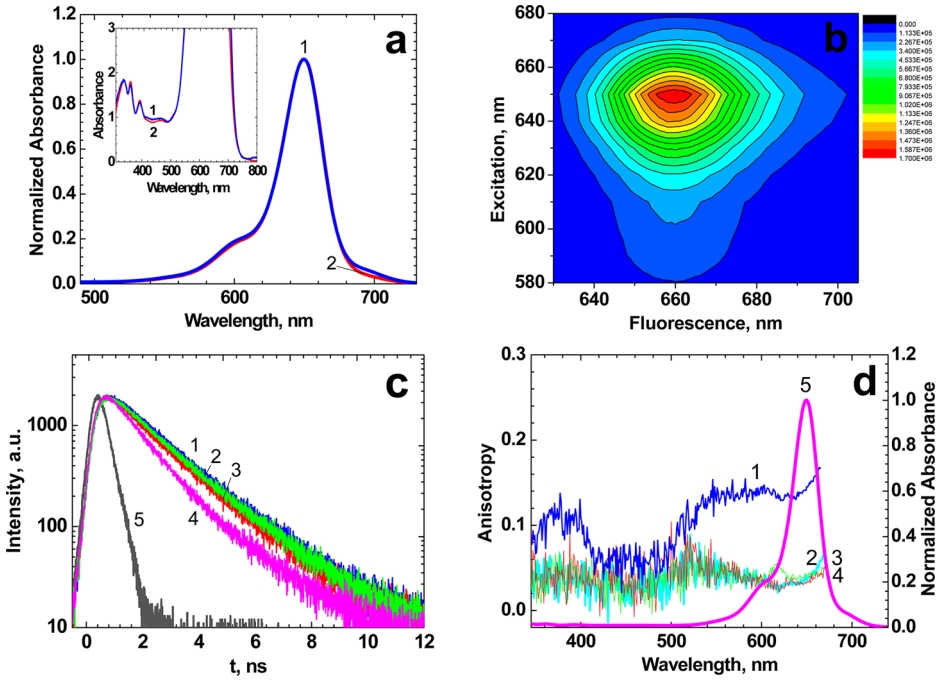

Figure 3. (a) Normalized 1PA spectra of **1** in THF for C = 10^{-6} M (1) and 10^{-3} M (2). The inset shows short wavelength absorption bands of **1** for the corresponding concentration. (b) 3D fluorescence map of **1** in TOL. (c) Fluorescence decay curves of **1** in TOL (1), THF (2), DCM (3), ACN (4), and instrument response function (5). (d) Excitation anisotropy spectra of **1** in pTHF (1), TOL (2), THF (3), DCM (4), and normalized 1PA spectrum in THF (5).

Table 1. Main Linear Spectroscopic and Photochemical Parameters of Branched Squaraine 1 in Solvents with Different Polarity Δf and Viscosity η: Absorption λ_{ab}^{max} and Fluorescence λ_{fl}^{max} Maxima, Stokes Shifts, Maximum Extinction Coefficients ε^{max}, Fluorescence Quantum Yields Φ_{fl}, Lifetimes τ_{fl}, and Photodecomposition Quantum Yields Φ_{ph}

N/N	TOL	THF	DCM	ACN
Δf[a]	0.0135	0.209	0.217	0.305
η, cP	0.59	0.48	0.4	0.34
λ_{ab}^{max}, nm	650 ± 1	650 ± 1	650 ± 1	646 ± 1
λ_{fl}^{max}, nm	661 ± 1	663 ± 1	662 ± 1	663 ± 1
Stokes shift, nm (cm^{-1})	11 ± 2 (260)	13 ± 2 (300)	12 ± 2 (280)	17 ± 2 (400)
$\varepsilon^{max}\cdot10^{-3}$, $M^{-1}\cdot cm^{-1}$	930 ± 50	860 ± 50	1020 ± 50	
Φ_{fl}	0.48 ± 0.03	0.36 ± 0.03	0.35 ± 0.03	0.05 ± 0.01
τ_{fl}, ns (A_i[b])	1.8 ± 0.1	1.7 ± 0.1	1.7 ± 0.1	1.2 ± 0.1 (90%) 3.3 ± 0.1 (10%)
$\Phi_{ph}\cdot10^{7}$	0.53 ± 0.1	3.1 ± 0.6	2.8 ± 0.6	

[a]Polarity (orientation polarizability) $\Delta f = [(\varepsilon - 1)/(2\varepsilon + 1)] - [(n^2 - 1)/(2n^2 + 1)]$, ε and n are the dielectric constant and refraction index of the solvent, respectively.[42] [b]A_i-relative amplitudes of corresponding decay.

electronically excited states. Solvent effects on the absorption spectra were taken into account with the Polarizable Continuum Model (PCM),[47] which accurately predicted solvatochromic shifts in previous studies.[48,49] The 2PA profiles were predicted with an in-house script,[50−52] implementing the sum over states (SOS) formalism[53] with 99 excited states. The necessary permanent dipole moments of the excited states were obtained with the modified Gaussian version.[54,48,55] The initial (before optimization) structure of **1** was chosen to have C_{3v} symmetry with all squaraine moieties at angles of 120 degrees. The DFTB geometry optimization made the structure unsymmetric, with two squaraine moieties nearly parallel, as shown in sec. 3.5. All conclusions in this paper are based on the unsymmetrical distribution.

3. RESULTS AND DISCUSSION

3.1. Linear Photophysics and Photostability of 1. The main linear spectroscopic characteristics and photochemical parameters of the star-shaped squaraine **1** are presented in Figures 2 and 3 and Table 1. The steady-state 1PA spectra of **1** were similar to corresponding centrosymmetric short squaraines,[11,56] and exhibited relatively narrow and sharp absorption contours (Figure 2a−c, curve 1), except for ACN where an additional H-aggregate absorbance[28] was observed at ≈606 nm (Figure 2d, curve 1) due to low solubility. In TOL, THF, and DCM solutions no aggregation effects were observed in the concentration range C ≤ 10^{-3} M (see, e.g., Figure 3a, curves 1 and 2). The maximum extinction coefficient, ε^{max}, of **1** was in the range of ∼10^6 $M^{-1}cm^{-1}$ (Table 1), which is one of the highest values ever reported for star-shaped or branched molecular structures, and may be of great interest for a number of practical applications, such as fluorescence bioimaging,[30] organic electronics,[3] etc. The similar spectral shape of the 1PA spectra of star-shaped **1** and a single squaraine molecule[11,56] allows one to assume the degenerate character of the main long wavelength absorption band of **1**. Also, the maximum value of the extinction

DOI: 10.1021/acs.jpcc.6b02446
J. Phys. Chem. C 2016, 120, 11099−11110

coefficient of **1** (~ (0.9−1.0)·10^6 M^{-1}cm^{-1}) is sufficiently close to a simple sum of corresponding ε^{max} for separate squaraine units (~ (0.3−0.4)·10^6 M^{-1}cm^{-1}), and does not give any evidence of cooperative electronic effects[57,58] between the three squaraine arms. The steady-state fluorescence spectra of **1** (Figure 2a−d, curve 2) exhibited small Stokes shifts, negligible solvatochromic behavior, and were independent of excitation wavelength, λ_{ex}, over the entire absorption band (see, for example, Figure 3b with typical 3D fluorescence map of **1** in TOL). It should be mentioned that corresponding dependence of the fluorescence spectrum of **1** in ACN on the excitation wavelength was not investigated due to aggregation effects.

The fluorescence quantum yield of **1**, Φ_{fl}, was also independent of λ_{ex} in all investigated solvents, i.e., all radiative transitions occurred from the lowest electronically excited state S_1 and no violations of Kasha's rule[42] were observed. In contrast to short centrosymmetric squaraine chromophores with four intramolecular hydrogen bonds (realized between squarate oxygens and hydroxyl groups),[11] star-shaped molecule **1** with the same type of squaraine arms exhibited a noticeable decrease in Φ_{fl} with increasing solvent polarity, Δf. This means that the observed dependence $\Phi_{fl} = f(\Delta f)$, can be explained by the solvent effect on the intramolecular (internal conversion) and/or intermolecular energy transfer (by Förster mechanism[42]) between the squaraine arms. It is worth mentioning that hydrogen bonding maintains the molecular structure of separate squaraine arms planar without any twisted intramolecular charge transfer (TICT) effects[59] that can lead to a decrease of Φ_{fl}. Fluorescence kinetics of **1** corresponded to a single exponential decay with corresponding lifetimes, $\tau_{fl} \approx 1.7-1.8$ ns, in all solvents (Figure 3c, curves 1−3), except for ACN (curve 4), where a double-exponential process was observed due to H-aggregation.

The steady-state excitation anisotropy spectra of **1** $r(\lambda)$ (Figure 3d, curves 1−4) revealed the nature of the long wavelength 1PA band. The values of $r(\lambda)$ noticeably changed in the spectral range of the main linear absorption band ~600−680 nm. These changes are indicative of at least two different electronic transitions that can be assigned to the main 1PA contour. This result is in contradiction with a C_3 symmetric geometrical model of **1**, which would be characterized by a fully degenerate nature of the main absorption band resulting from the three symmetrically oriented squaraine chromophores. Based on the experimental excitation anisotropy spectra, we can assume preferential energy stabilization of one of the squaraine arms of **1** relative to the other arms, resulting in a change of the optimized molecular geometry and corresponding symmetry breaking in the ground electronic state S_0. This effect was previously observed and comprehensively analyzed for symmetrical triphenylmethane derivatives,[60] and for longer cyanine derivatives.[61−63] Relatively low absolute values of the fundamental excitation anisotropy in the main 1PA band, $r_0(\lambda) \approx 0.13-0.17$ (see Figure 3d, curve 1) also confirm this assumption, and can be an indication of efficient intramolecular energy redistribution between squaraine arms. Similar effects were reported for star-shaped octupolar chromophores in polymeric media.[64]

In low viscosity solvents (TOL, THF, DCM) the excitation anisotropy values noticeably decreased due to rotational movement of **1** (Figure 3d, curves 2−4). The rotational correlation times, θ, and effective rotational molecular volumes, V, of **1** were determined for each solvent using eq 1 and corresponding parameters η and τ_{fl} from Table 1. The obtained values of θ and V are presented in Table 2 for solvents of different polarity. According to this data, the effective rotational molecular volume V increases with Δf, giving evidence of increased solute−solvent interactions in polar media, where a much larger number of relatively small solvent molecules is involved in the rotational moment of **1**. The effect of strong solute−solvent interactions in polar media can also be related to the observed dependence $\Phi_{fl} = f(\Delta f)$, which is discussed above.

Table 2. Excitation Anisotropy at λ_{ab}^{max}, Rotational Correlation Time θ, and Effective Rotational Molecular Volume V of 1 in Solvents of Different Polarity Δf

N/N	TOL	THF	DCM
$r(\lambda_{ab}^{max})$	0.035	0.036	0.036
θ, ns	0.62	0.61	0.61
V, Å^3	4400	5300	6300
Δf	0.0135	0.209	0.217

The photochemical stability of **1** was investigated at room temperature in the majority of the employed solvents in order to evaluate its potential for practical use. It should be emphasized that we performed quantitative determination of photostability as the photodecomposition quantum yield, Φ_{ph}, is a molecular parameter (i.e., independent of experimental conditions), in contrast to relative kinetic absorption/emission photochemical measurements typically presented in the majority of scientific reports (see, e.g., refs. 35, 65, and 66). The values of Φ_{ph} were obtained by a previously developed absorption method[44] and are presented in Table 1. The highest level of photostability ($\Phi_{ph} \approx 5\cdot10^{-8}$) was observed for TOL solution of **1** that is at least 2 orders of magnitude higher in comparison with the best laser dyes.[67−69] The value of Φ_{ph} noticeably increases in solvents of higher polarity (THF and DCM), but still remains in the range of practical applicability. It should be mentioned that first order photochemical reaction processes[70] were revealed from the photodecomposition kinetic changes in the absorption spectra of **1** in all the investigated solvents. The photostability data indicates that star-shaped squaraine **1** holds substantial promise as a probe in bioimaging applications.

3.2. 2PA Spectral Properties of Star-Shaped Squaraine 1.

The degenerate 2PA spectrum of **1** was obtained in THF over a broad spectral range using an open aperture Z-scan technique[45] with a 1 kHz femtosecond laser and is shown in Figure 4 (curve 1). The shape of the obtained 2PA spectrum revealed two maxima at ≈820 nm and ≈1200 nm, and was very similar to the corresponding one for the single centrosymmetric squaraine unit

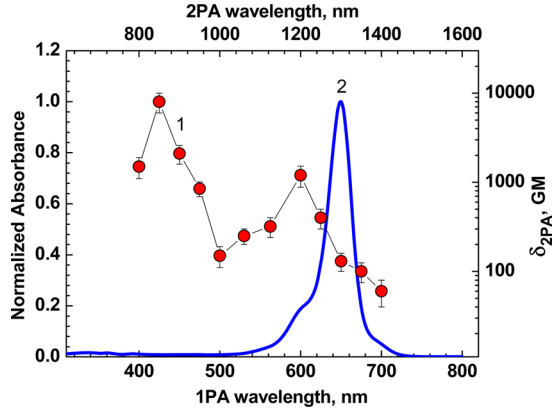

Figure 4. Degenerate 2PA (1) and normalized 1PA (2) spectra of **1** in THF.

DOI: 10.1021/acs.jpcc.6b02446
J. Phys. Chem. C 2016, 120, 11099−11110

with four intramolecular hydrogen bonds,[11] except for its absolute magnitude. The molecular structure of separate squaraine arms in **1** appears close to centrosymmetric, thus one cannot expect large two-photon absorption cross sections, δ_{2PA}, in the main one-photon allowed linear absorption band. Relatively weak 2PA efficiency ($\delta_{2PA} \sim 100$ GM) was observed in this spectral range with a noticeable increase to ~1000 GM (long wavelength 2PA maximum) at the vibrational shoulder of the 1PA contour (at ≈600 nm). This is evidence of vibronic coupling with asymmetrical vibration modes,[11,21,71] which violates the selection rules.[72,73] The most intense short wavelength 2PA maximum with $\delta_{2PA} \approx 8000$ GM (at ≈820 nm) corresponded to the spectral range of the lowest 1PA (see insert in Figure 3a) and two-photon allowed $S_0 \rightarrow S_n$ transitions (S_0 and S_n are the ground and high excited electronic states of **1**, respectively). The nature of the short wavelength 2PA band can be analyzed using the simplest three-level energy model[74] based on the sum-over-states (SOS) approach,[53] when δ_{2PA} is determined by the expression:

$$\delta_{2PA} \sim \frac{E_P^2 \times |\boldsymbol{\mu}_{01}|^2 \times |\boldsymbol{\mu}_{1n}|^2}{((E_{01} - E_P)^2 + \Gamma_{01}^2) \times ((E_{0n} - 2E_P)^2 + \Gamma_{0n}^2)}$$

where $E_P = hc/\lambda_{ex}$ (h and c are Planck's constant and the velocity of light in vacuum, respectively); $E_{01} = hc/\lambda_{ab}^{max}$; $\boldsymbol{\mu}_{01}$ and $\boldsymbol{\mu}_{1n}$ are the transition dipoles of $S_0 \rightarrow S_1$ and $S_1 \rightarrow S_n$ electronic transitions, respectively; E_{0n} is the energy of the final electronic state S_n; Γ_{01} and Γ_{0n} are the damping factors of the corresponding transitions. The value of the transition dipole μ_{01} is directly related to the integral of the 1PA spectrum of **1**, $\mu_{01} \approx 0.096 \times \sqrt{\int \varepsilon(\nu) \times d\nu/\nu^{max}}$ (where $\nu = 1/\lambda_{ab}^{max}$),[75] with an extremely large maximum extinction coefficient $\varepsilon(\lambda_{ab}^{max}) \sim 10^6$ $M^{-1}cm^{-1}$. Also, the relatively small detuning energy, $\Delta E = E_{01} - E_P$, leads to intermediate state resonance enhancement (ISRE),[76] and a corresponding "double resonance" excitation condition[77] for the $S_0 \rightarrow S_n$ two-photon transition when $E_{0n} = 2E_P$. Apparently, these parameters are mainly responsible for so large a two-photon cross section δ_{2PA} in the short wavelength 2PA band of **1**. It is interesting that the branched squaraine **1** is characterized by more than a 2 times enhancement of δ_{2PA}, relative to a simple sum of the corresponding maximum cross sections of separate squaraine units with $\delta_{2PA} \sim 1000$ GM.[11] Presumably, this enhancement is related to the resonance excitation conditions without a noticeable role of cooperative effects.[57,58]

Acceptable fluorescence quantum yield, large 2PA cross sections and extremely high photostability reveal the potential of **1** for 2PFM applications that can be quantitatively characterized by the "figure of merit", $F_M = \delta_{2PA} \times \Phi_{fl}/\Phi_{ph}$.[1] The calculated values of $F_M \sim 10^{10}-10^{11}$ GM for squaraine **1** strongly exceed the values of other known two-photon fluorescent labels.[11,78]

3.3. Femtosecond Transient Absorption Spectroscopy of Star-Shaped Squaraine 1. The transient absorption and gain properties of **1** were investigated in TOL at room temperature by the femtosecond pump−probe method,[38,79] as described in sec. 2.3 and schematically shown in Figure 5. The sample solution of **1** was excited in the main 1PA band at λ_{ex} = 650 nm and the value of the induced optical density, ΔD, was measured by a weak probe pulse as a function of temporal delay, τ_D, between pump and probe pulses. Typical dependences $\Delta D = f(\tau_D)$ are presented in Figure 6a−c for selected probing wavelengths, λ_{pr}. As follows from the obtained kinetic curves

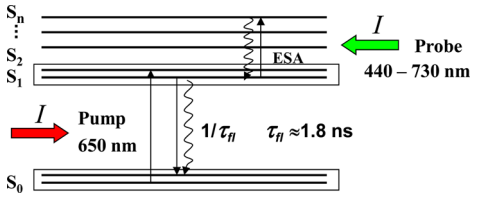

Figure 5. Schematic diagram of the simplified electronic model of **1** and main spontaneous and stimulated transitions (see text for details).

$\Delta D = f(\tau_D)$, the absolute values of ΔD exhibited fast relaxations with characteristic times of 3−4 ps and then (for τ_D > 10−15 ps) slowly decreased to zero in accordance with the nanosecond lifetime of the S_1 state. The fast relaxation processes can be attributed to the solvent reorganization phenomena in the solvate cage of **1** after electronic excitation $S_0 \rightarrow S_1$ that are typically observed for low viscosity dye solutions at room temperature.[42,80] It is interesting that fast solvent relaxations were not observed for single squaraine units under similar excitation conditions,[11] which can be evidence of a solvent dependent energy redistribution between squaraine arms in the branched molecule **1**. These data also support the assumption of symmetry breaking in the S_0 state of **1** as a result of the preferential energy stabilization of one of the squaraine arms in the molecular structure relative to other two.[60] The transient absorption (TA) spectrum of **1** was obtained over a broad spectral range and two well-defined maxima were revealed at ≈500 and 650 nm, respectively (Figure 6d, curve 1). In general, the nature of the TA spectrum and corresponding kinetic curves can be related to saturable absorption (SA), excited state absorption (ESA), and gain (light amplification) processes, typically observed in TA pump−probe molecular spectroscopy.[68] The short wavelength TA band with a maximum at ~500 nm corresponds to the spectral range of zero gain and extremely weak linear absorbance (see Figures 3a and 6d, curves 2 and 3), and therefore, can be assigned to pure ESA processes. It should be mentioned that the short wavelength ESA band of **1** corresponds well with the known ESA spectra of similar symmetrical squaraine derivatives with $\lambda_{ab}^{max} \approx 630-650$ nm.[11,32] The dependence of $\Delta D = f(\tau_D)$ for λ_{pr} = 500 nm (Figure 6a) revealed temporal changes in the instantaneous short wavelength ESA contour and can be assigned to solvent relaxation processes in the S_1 state of **1**. The kinetic curve for λ_{pr} = 650 nm ≈ λ_{ab}^{max} (Figure 6b) exhibited the largest negative values of ΔD, which was mainly due to the depopulation of the ground state S_0 (i.e., by SA processes). We can assume an additional ESA contribution to this value of ΔD at λ_{pr} = 650 nm, which is characterized by the fast transient changes observed at pump−probe delays of τ_D > 300−350 fs, and is related to solvate relaxation processes in the S_1 state. It should be emphasized that ground state depopulation occurs with a constant solvate configuration of **1** in the S_0 state and no fast relaxations should be observed for induced changes in the ground state absorption for $\tau_D \ll \tau_{fl}$. The kinetic curve for λ_{pr} = 670 nm (Figure 6c) revealed a small amplitude of the fast relaxation component in ΔD (i.e., fast changes from ≈ −0.028 to ≈ −0.024 in the first 2−3 ps after excitation), and a relatively large relaxed negative value (i.e., ≈ −0.024) in the spectral range of the fluorescence maximum of **1** (Figure 6d, curve 1). The negative value of ΔD at $\lambda_{pr} \approx \lambda_{fl}^{max}$ noticeably exceeds the estimated value of the corresponding transient absorbance related to possible SA effects at this probe wavelength. This is evidence of gain (optical amplification). Based on this result, we can expect super-

DOI: 10.1021/acs.jpcc.6b02446
J. Phys. Chem. C 2016, 120, 11099−11110

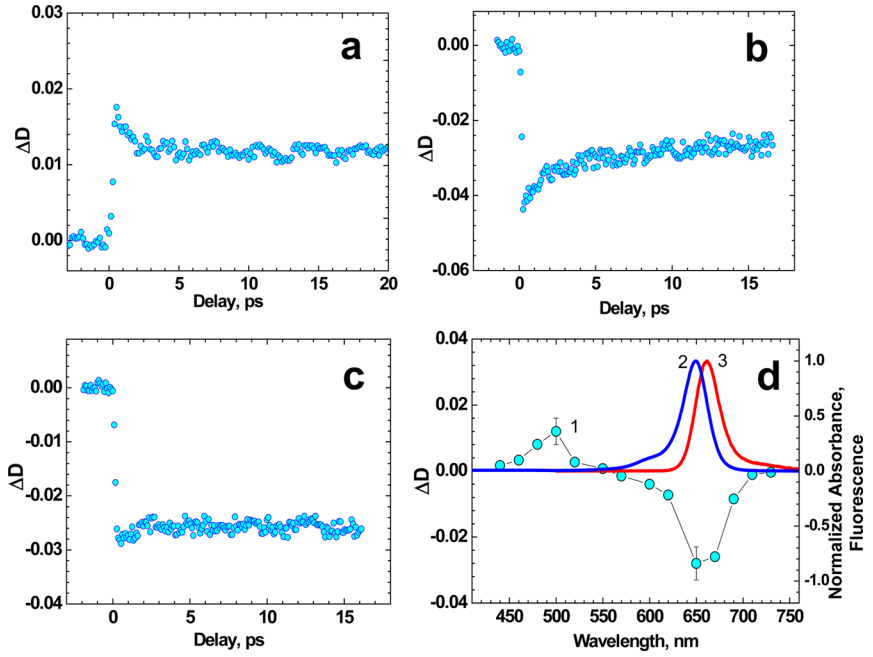

Figure 6. (a–c) The dependences $\Delta D = f(\tau_D)$ for **1** in TOL: λ_{pr} = 500 nm (a), 650 nm (b), and 670 nm (c). (d) Transient absorption spectrum for $\tau_D \approx$ 15 ps (1), normalized steady-state absorption (2), and fluorescence (3) spectra of **1** in TOL.

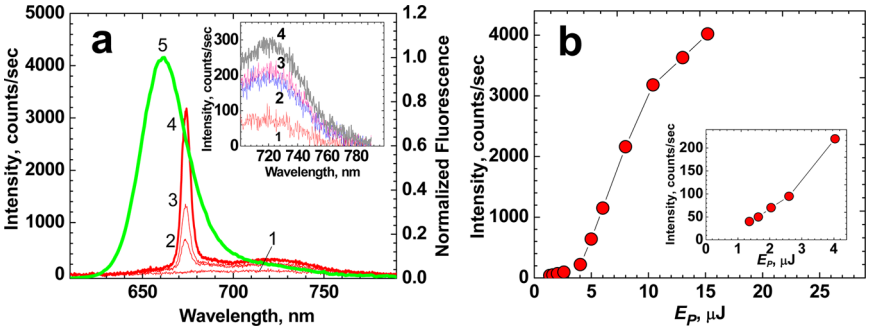

Figure 7. (a) The superluminescence bands and reabsorbed spontaneous fluorescence emission spectra of **1** (see inset with corresponding extended range of intensity) in TOL at C ≈ 2.3 × 10^{-4} M under femtosecond pumping with pulse energy$E_P \approx$ 1.4 μJ (1), 5 μJ (2), 6 μJ (3), 10 μJ (4), and normalized steady-state fluorescence spectrum of **1** in TOL for C ≈ 10^{-7} M (5). (b) The dependence of the integrated emission intensity, *I*, on E_P at C ≈ 2.3 × 10^{-4} M. The inset in (b) shows corresponding initial part of the dependence $I = f(E_P)$.

luminescence and lasing properties of **1**, which are attractive for fluorescence microscopy applications and will be described in the next section.

3.4. Superluminescent Properties of Star-Shaped Squaraine 1. The potential abilities of organic molecules for superluminescence and random lasing in a highly scattering media[81,82] is a subject of increasing interest for bioimaging applications due to the increased spectral brightness from stimulated emission.[83] Efficient superluminescence of **1** was observed at room temperature in relatively low concentrated TOL solution (C ≈ 2.3·10^{-4} M) under one-photon femtosecond transverse pumping into the main long wavelength absorption band (Figure 7). The broad spontaneous fluorescence emission spectrum of **1** (Figure 7a) was highly reabsorbed at C ∼ 10^{-4} M and a relatively narrow superluminescence band (fwhm ∼8–10 nm) arose with an increase in pumping energy, E_P. The dependence of the integral emission intensity, *I*, on E_P revealed an obvious threshold character (Figure 7b) with corresponding threshold value, $E_P^{th} \approx 3$ μJ/pulse. The dependence $I = f(E_P)$ was approximately linear for $E_P < E_P^{th}$ (see insert in Figure 7b) and saturated under E_P > 7–8 μJ. The nature of this saturation is related with the noticeable increase in the spatial divergence of the superfluorescence pulse when some part of its energy misses the photodetector due to thermooptical distortions in the active medium. It should be emphasized that, besides the obvious intensity threshold, the observed emission was linearly polarized (parallel to the pumping polarization) and exhibited relatively low spatial divergence ∼3–4 mrad (at $E_P \leq 7$ μJ), which is typical for stimulated emission in organic dye solutions.[83] Superluminescence of **1** is a promising molecular property for the development of new fluorescent labels with increased spectral brightness.

3.5. Quantum Chemical Calculations of the Electronic Properties of Branched Squaraine 1. The DFTB optimized structure of **1** is shown in Figure 8. As follows from these data, geometry optimization made the starting symmetrical (C_{3v} symmetry) branched squaraine structure asymmetric with the angles of ≈28°, ≈ 60°, and ≈73° between corresponding squaraine moieties. Both 1PA and 2PA spectra predicted by ZINDO/S level of theory are shown in Figure 9 and relatively good agreement with the corresponding experimental data can be observed (see Figure 2). The main parameters of the essential

DOI: 10.1021/acs.jpcc.6b02446
J. Phys. Chem. C 2016, 120, 11099–11110

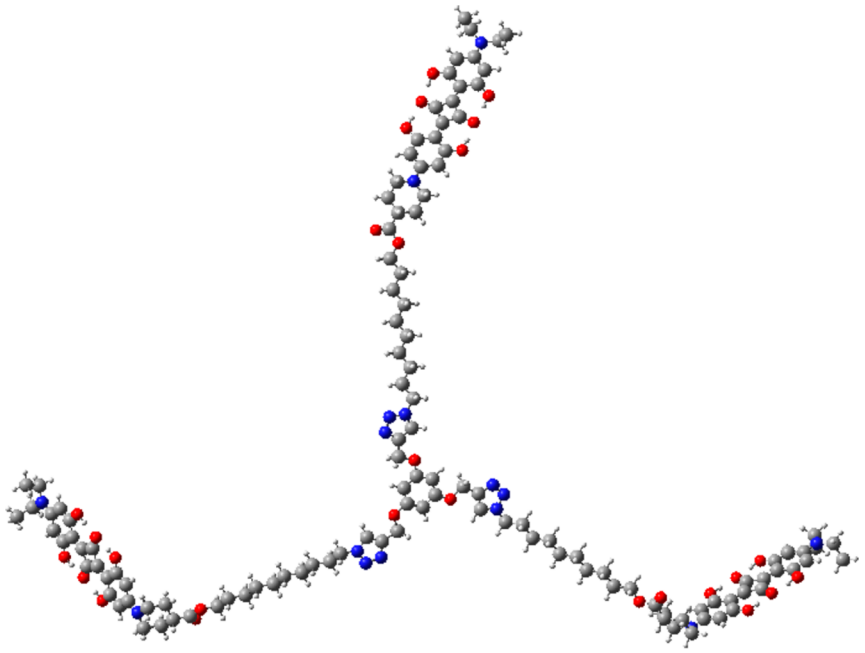

Figure 8. Optimized structure of **1** at the DFTB level of theory.

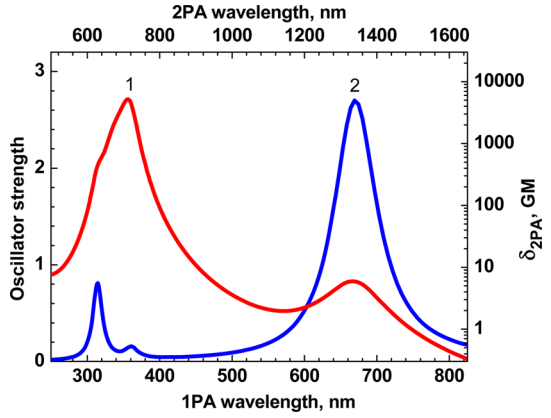

Figure 9. Calculated degenerate 2PA (1) and linear 1PA (2) spectra of **1**. Curves 1 and 2 were obtained using the Lorentz line shape function with 0.1 eV for the damping parameter Γ.

excited states and corresponding molecular orbitals of **1** are presented in Table 3 and Figure 10, respectively. The low wavelength 1PA peak is an overlap of the absorption from the nearly degenerate states S_1, S_2, and S_3, while the higher energy peak is an overlap from S_{10}, S_{11}, and S_{12}. All these states along with S_0 have negligible permanent dipole moments, that were nicely reflected in the extremely weak solvatochromic behavior of **1**. The 2PA band corresponds to absorption into the S_7, S_8, and S_9 states, which are strongly polar. Each of these 2PA states is dominated by a single configuration, corresponding to the local excitation in one squaraine chromophore. In contrast, 1PA states are nearly an equal mix of all three local excitations. It should be mentioned that the proposed theoretical approach nicely described the majority of the linear and nonlinear optical properties of **1**.

4. CONCLUSIONS

Comprehensive linear photophysical, photochemical, and nonlinear optical investigations of a novel three-armed star-shaped squaraine (**1**) with four intramolecular hydrogen bonds were performed in a number of organic solvents at room temperature. The steady-state linear 1PA spectra of **1** showed relatively narrow, sharp peaks, and exhibited extremely large extinction coefficients ($\sim 10^6$ $M^{-1}cm^{-1}$) and a weak dependence on solvent properties. The steady-state fluorescence spectra of **1** were independent of λ_{ex} over the entire absorption range, exhibiting small Stokes shifts and negligible solvatochromic behavior. The excitation anisotropy spectra of **1**, along with the noticeable

Table 3. Essential Excited States: Wavelengths (nm), Oscillator Strength (osc.), Calculated 2PA Cross Sections (GM), Permanent Dipole Moments (a.u.), and the Contributions of the Leading Configurations (H = HOMO, L = LUMO, etc)

	nm	osc.	2PA	μ_x	μ_y	μ_z	
S1	672	1.06	1	−0.1	0.1	0.1	−0.13(H-2→L)−0.44(H-1→L+1)+0.54(H→L+2)
S2	671	0.43	1	−0.1	0.2	0.1	−0.34(H-2→L)+0.52(H-1→L+1)+0.34(H→L+2)
S3	670	2.70	3	−0.2	0.1	0.1	0.61(H-2→L)+0.20(H-1→L+1)+0.31(H→L+2)
S7	359	0.02	2204	−10.5	6.0	7.4	−0.18(H-8→L)+0.68(H-5→L)
S8	358	0.02	1179	−13.3	4.6	1.8	0.61(H-7→L+2)-0.34(H-4→L+2)0.10(H→L+5)
S9	358	0.02	1181	2.8	10.4	9.3	0.61(H-6→L+1)−0.34(H-3→L+1)−0.10(H-1→L+4)
S10	314	0.28	85	0.0	0.1	0.1	−0.15(H-2→L)+0.65(H-1→L+1)+0.23(H→L+2)
S11	314	0.56	46	−0.1	0.0	0.0	−0.15(H-4→L+2)−0.23(H-1→L+4)+0.65(H→L + 5)
S12	314	0.40	108	0.0	0.0	0.0	0.13(H-5→L)+0.69(H-2→L+3)

DOI: 10.1021/acs.jpcc.6b02446
J. Phys. Chem. C 2016, 120, 11099−11110

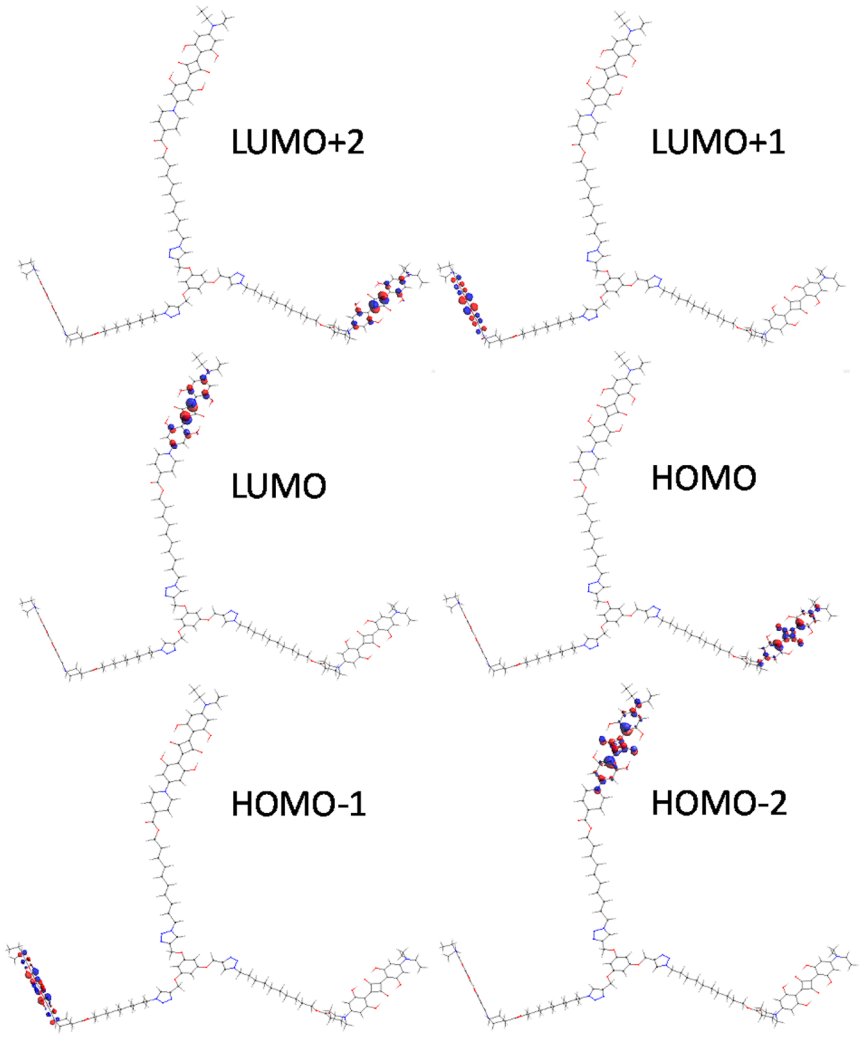

Figure 10. Main molecular orbitals for **1** obtained at the ZINDO/S level of theory.

dependence of the fluorescence quantum yield on solvent polarity, revealed the effect of symmetry breaking in the ground electronic state of the star-shaped molecular structure. The degenerate 2PA spectrum of **1** was obtained over a broad spectral range by open aperture Z-scans and exhibited a maximum cross section $\delta_{2PA} \approx 8000$ GM in the short wavelength two-photon-allowed band. Noticeable enhancement of 2PA efficiency per squaraine arm was observed in **1** relative to separate single squaraine units. The nature of fast dynamic processes in the excited states of **1** was revealed using a femtosecond transient absorption pump−probe technique and corresponding relaxation times of 3−4 ps were shown which can be assigned to solvent molecular interactions. Efficient superluminescent emission of **1** was observed in relatively low concentration toluene solution under femtosecond pumping. The electronic structure, linear, and nonlinear optical properties of **1** were predicted with semiempirical quantum-chemical calculations. The calculated 1PA and 2PA spectra were in good agreement with experimental data. Good values of fluorescence quantum yield, extremely high photostability, large 2PA cross sections and superluminescence properties determine the potential of the star-shaped squaraine **1** for use in 2PFM applications, including bioimaging, aspects to be investigated in future studies.

■ ASSOCIATED CONTENT

Supporting Information

The Supporting Information is available free of charge on the ACS Publications website at DOI: 10.1021/acs.jpcc.6b02446.

Materials and methods used, synthesis of compounds **1**−**1-5**, synthesis of dyes **1-6** and **1**, and ^{1}H and ^{13}C NMR spectra (PDF)

■ AUTHOR INFORMATION

Corresponding Authors

*E-mail: mbondar@mail.ucf.edu; Tel: 38-044-525-9968.
*E-mail: belfield@njit.edu; Tel: 1-973-596-3676.
*E-mail: ewvs@creol.ucf.edu; Tel: 1-407-823-6835.

Notes

The authors declare no competing financial interest.

■ ACKNOWLEDGMENTS

We wish to acknowledge the National Science Foundation (CBET-1517273 and CHE-0832622), the National Academy of Sciences of Ukraine (grant VC/157), and FP7-Marie Curie Actions: ITN "Nano2Fun" GA #607721. Calculations were performed using UCF Advanced Research Computing Center, and supported by the Russian Science Foundation, Contract No. 14−43−00052. E.V.S. and D.J.H. thank the support of the

DOI: 10.1021/acs.jpcc.6b02446
J. Phys. Chem. C 2016, 120, 11099−11110

National Science foundation (ECCS-1202471 and ECCS-1229563) and the Air Force Office of Scientific Research MURI grant FA9550-10-1-0558.

REFERENCES

(1) Wang, X.; Nguyen, D. M.; Yanez, C. O.; Rodriguez, L.; Ahn, H.-Y.; Bondar, M. V.; Belfield, K. D. High-Fidelity Hydrophilic Probe for Two-Photon Fluorescence Lysosomal Imaging. *J. Am. Chem. Soc.* **2010**, *132* (35), 12237−12239.

(2) Yang, D.; Zhu, Y.; Jiao, Y.; Yang, L.; Yang, Q.; Luo, Q.; Pu, X.; Huang, Y.; Zhao, S.; Lu, Z. N,N-Diarylamino End-Capping as a New Strategy for Simultaneously Enhancing Open-Circuit Voltage, Short-Circuit Current Density and Fill Factor in Small Molecule Organic Solar Cells. *RSC Adv.* **2015**, *5*, 20724−20733.

(3) Bellani, S.; Iacchetti, A.; Porro, M.; Beverina, L.; Antognazza, M. R.; Natali, D. Charge Transport Characterization in a Squaraine-Based Photodetector by Means of Admittance Spectroscopy. *Org. Electron.* **2015**, *22*, 56−61.

(4) Maeda, T.; Nitta, S.; Nakao, H.; Yagi, S.; Nakazumi, H. Squaraine Dyes with Pyrylium and Thiopyrylium Components for Harvest of near Infrared Light in Dye-Sensitized Solar Cells. *J. Phys. Chem. C* **2014**, *118*, 16618−16625.

(5) Emmelius, M.; Pawlowski, G.; Vollmann, H. W. Materials for Optical Data Storage. *Angew. Chem.* **1989**, *101* (11), 1475−502.

(6) Jipson, V. B.; Jones, C. R. Infrared Dyes for Optical Storage. *J. Vac. Sci. Technol.* **1981**, *18* (1), 105−109.

(7) Lee, S.; Rao, B. A.; Son, Y.-A. A Highly Selective Fluorescent Chemosensor for Hg^{2+} Based on Asquaraine-Bis(Rhodamine-B) Derivative: Part Ii. *Sens. Actuators, B* **2015**, *210*, 519−532.

(8) Ajayaghosh, A. Chemistry of Squaraine-Derived Materials: Near-Ir Dyes, Low Band Gap Systems, and Cation Sensors. *Acc. Chem. Res.* **2005**, *38* (6), 449−459.

(9) Hsueh, S.-Y.; Lai, C.-C.; Liu, Y.-H.; Wang, Y.; Peng, S.-M.; Chiu, S.-H. Protecting a Squaraine near-Ir Dye through Its Incorporation in a Slippage-Derived [2]Rotaxane. *Org. Lett.* **2007**, *9* (22), 4523−4526.

(10) Webster, S.; Fu, J.; Padilha, L. A.; Przhonska, O. V.; Hagan, D. J.; Van Stryland, E. W.; Bondar, M. V.; Slominsky, Y. L.; Kachkovski, A. D. Comparison of Nonlinear Absorption in Three Similar Dyes: Polymethine, Squaraine and Tetraone. *Chem. Phys.* **2008**, *348*, 143−151.

(11) Belfield, K. D.; Bondar, M. V.; Haniff, H. S.; Mikhailov, I. A.; Luchita, G.; Przhonska, O. V. Superfluorescent Squaraine with Efficient Two-Photon Absorption and High Photostability. *ChemPhysChem* **2013**, *14*, 3532−3542.

(12) Chen, C.-T.; Marder, S. R.; Cheng, L.-T. Syntheses and Linear and Nonlinear Optical Properties of Unsymmetrical Squaraines with Extended Conjugation. *J. Am. Chem. Soc.* **1994**, *116* (7), 3117−3118.

(13) Beverina, L.; Crippa, M.; Landenna, M.; Ruffo, R.; Salice, P.; Silvestri, F.; Versari, S.; Villa, A.; Ciaffoni, L.; Collini, E.; et al. Assessment of Water-Soluble π-Extended Squaraines as One- and Two-Photon Singlet Oxygen Photosensitizers: Design, Synthesis, and Characterization. *J. Am. Chem. Soc.* **2008**, *130*, 1894−1902.

(14) Avirah, R. R.; Jayaram, D. T.; Adarsh, N.; Ramaiah, D. Squaraine Dyes in Pdt: From Basic Design to in Vivo Demonstration. *Org. Biomol. Chem.* **2012**, *10*, 911−920.

(15) Luo, C.; Zhou, Q.; Jiang, G.; He, L.; Zhang, B.; Wang, X. The Synthesis and $^1O_2$ Photosensitization of Halogenated Asymmetric Aniline-Based Squaraines. *New J. Chem.* **2011**, *35*, 1128−1132.

(16) Escobedo, J. O.; Rusin, O.; Lim, S.; Strongin, R. M. NIR Dyes for Bioimaging Applications. *Curr. Opin. Chem. Biol.* **2010**, *14*, 64−70.

(17) Cole, E. L.; Arunkumar, E.; Xiao, S.; Smith, B. A.; Smith, B. D. Water-Soluble, Deep-Red Fluorescent Squaraine Rotaxanes. *Org. Biomol. Chem.* **2012**, *10*, 5769−5773.

(18) Podgorski, K.; Terpetschnig, E.; Klochko, O. P.; Obukhova, O. M.; Haas, K. Ultra-Bright and -Stable Red and near-Infrared Squaraine Fluorophores for in Vivo Two-Photon Imaging. *PLoS One* **2012**, *7* (12), e51980.

(19) Beverina, L.; Salice, P. Squaraine Compounds: Tailored Design and Synthesis Towards a Variety of Material Science Applications. *Eur. J. Org. Chem.* **2010**, *2010* (7), 1207−1225.

(20) Sreejith, S.; Carol, P.; Chithra, P.; Ajayaghosh, A. Squaraine Dyes: A Mine of Molecular Materials. *J. Mater. Chem.* **2008**, *18*, 264−274.

(21) Scherer, D.; Dorfler, R.; Feldner, A.; Vogtmann, T.; Schwoerer, M.; Lawrentz, U.; Grahn, W.; Lambert, C. Two-Photon States in Squaraine Monomers and Oligomers. *Chem. Phys.* **2002**, *279*, 179−207.

(22) Odom, S. A.; Webster, S.; Padilha, L. A.; Peceli, D.; Hu, H.; Nootz, G.; Chung, S. J.; Ohira, S.; Matichak, J. D.; Przhonska, O. V.; et al. Synthesis and Two-Photon Spectrum of a Bis(Porphyrin)-Substituted Squaraine. *J. Am. Chem. Soc.* **2009**, *131* (22), 7510−7511.

(23) Beverina, L.; Ruffo, R.; Salamone, M. M.; Ronchi, E.; Binda, M.; Natali, D.; Sampietro, M. Panchromatic Squaraine Compounds for Broad Band Light Harvesting Electronic Devices. *J. Mater. Chem.* **2012**, *22*, 6704−6710.

(24) Umezawa, K.; Citterio, D.; Suzuki, K. Water-Soluble Nir Fluorescent Probes Based on Squaraine and Their Application for Protein Labeling. *Anal. Sci.* **2008**, *24*, 213−217.

(25) Paek, S.; Choi, H.; Kim, C.; Cho, N.; So, S.; Song, K.; Nazeeruddin, M. K.; Ko, J. Efficient and Stable Panchromatic Squaraine Dyes for Dye-Sensitized Solar Cells. *Chem. Commun.* **2011**, *47*, 2874−2876.

(26) Pisoni, D. S.; Petzhold, C. L.; de Abreu, M. P.; Rodembusch, F. S.; Campo, L. F. Synthesis, Spectroscopic Characterization and Photophysical Study of Dicyanomethylene Substituted Squaraine Dyes. *C. R. Chim.* **2012**, *15*, 454−462.

(27) Sun, C.-L.; Liao, Q.; Li, T.; Li, J.; Jiang, J.-Q.; Xu, Z.-Z.; Wang, X.-D.; Shen, R.; Bai, D.-C.; Wang, Q.; et al. Rational Design of Small Indolic Squaraine Dyes with Large Two-Photon Absorption Cross Section. *Chem. Sci.* **2015**, *6*, 761−769.

(28) Mayerhoffer, U.; Wurthner, F. Cooperative Self-Assembly of Squaraine Dyes. *Chem. Sci.* **2012**, *3*, 1215−1220.

(29) Beverina, L.; Drees, M.; Facchetti, A.; Salamone, M.; Ruffo, R.; Pagani, G. A. Bulk Heterojunction Solar Cells − Tuning of the Homo and Lumo Energy Levels of Pyrrolic Squaraine Dyes. *Eur. J. Org. Chem.* **2011**, *2011*, 5555−5563.

(30) Ahn, H.-Y.; Yao, S.; Wang, X.; Belfield, K. D. Near-Infrared-Emitting Squaraine Dyes with High 2PA Cross-Sections for Multiphoton Fluorescence Imaging. *ACS Appl. Mater. Interfaces* **2012**, *4*, 2847−2854.

(31) Chung, S.-J.; Zheng, S.; Odani, T.; Beverina, L.; Fu, J.; Padilha, L. A.; Biesso, A.; Hales, J. M.; Zhan, X.; Schmidt, K.; et al. Extended Squaraine Dyes with Large Two-Photon Absorption Cross-Sections. *J. Am. Chem. Soc.* **2006**, *128*, 14444−14445.

(32) Webster, S.; Peceli, D.; Hu, H.; Padilha, L. A.; Przhonska, O. V.; Masunov, A. E.; Gerasov, A. O.; Kachkovski, A. D.; Slominsky, Y. L.; Tolmachev, A. I.; et al. Near-Unity Quantum Yields for Intersystem Crossing and Singlet Oxygen Generation in Polymethine-Like Molecules: Design and Experimental Realization. *J. Phys. Chem. Lett.* **2010**, *1*, 2354−2360.

(33) Qaddoura, M. A.; Belfield, K. D.; Tongwa, P.; DeSanto, J. E.; Timofeeva, T. V.; Heiney, P. A. Thermotropic Behaviour, Self-Assembly and Photophysical Properties of a Series of Squaraines. *Supramol. Chem.* **2011**, *23* (11), 731−742.

(34) Cornelissen-Gude, C.; Rettig, W.; Lapouyade, R. Photophysical Properties of Squaraine Derivatives: Evidence for Charge Separation. *J. Phys. Chem. A* **1997**, *101*, 9673−9677.

(35) Terpetschnig, E.; Szmacinski, H.; Lakowicz, J. R. An Investigation of Squaraines as a New Class of Fluorophores with Long-Wavelength Excitation and Emission. *J. Fluoresc.* **1993**, *3* (3), 153−155.

(36) Borisevich, N. A. Polarization of Spontaneous and Stimulated Radiation of Complex Molecules in the Gas Phase. *J. Lumin.* **1979**, *18*−*19*, 127−130.

(37) Nenchev, M. N. Cavity Configuration in a Dye Laser for Dispersion on the Two Output Beams. *Opt. Commun.* **1984**, *50* (1), 36−40.

(38) Belfield, K. D.; Bondar, M. V.; Morales, A. R.; Yue, X.; Luchita, G.; Przhonska, O. V. Transient Excited-State Absorption and Gain

DOI: 10.1021/acs.jpcc.6b02446
J. Phys. Chem. C 2016, 120, 11099−11110

Spectroscopy of a Two-Photon Absorbing Probe with Efficient Superfluorescent Properties. *J. Phys. Chem. C* **2012**, *116*, 11261−11271.
(39) Belfield, K. D.; Bondar, M. V.; Yao, S.; Mikhailov, I. A.; Polikanov, V. S.; Przhonska, O. V. Femtosecond Spectroscopy of Superfluorescent Fluorenyl Benzothiadiazoles with Large Two-Photon and Excited-State Absorption. *J. Phys. Chem. C* **2014**, *118*, 13790−13800.
(40) Zheng, G.; Witek, H. A.; Bobadova-Parvanova, P.; Irle, S.; Musaev, D. G.; Prabhakar, R.; Morokuma, K.; et al. Parameter Calibration of Transition-Metal Elements for the Spin-Polarized Self-Consistent-Charge Density-Functional Tight-Binding (DFTB) Method: Sc, Ti, Fe, Co, and Ni. *J. Chem. Theory Comput.* **2007**, *3* (4), 1349−1367.
(41) Zerner, M. C.; Loew, G. H.; Kirchner, R. F.; Muellerwesterhoff, U. T. Intermediate Neglect of Differential-Overlap Technique for Spectroscopy of Transition-Metal Complexes - Ferrocene. *J. Am. Chem. Soc.* **1980**, *102* (2), 589−599.
(42) Lakowicz, J. R. *Principles of Fluorescence Spectroscopy*; Kluwer: New York, 1999.
(43) Magde, D.; Brannon, J. H.; Cremers, T. L.; Olmsted, J., III Absolute Luminescence Yield of Cresyl Violet. A Standard for the Red. *J. Phys. Chem.* **1979**, *83* (6), 696−699.
(44) Corredor, C. C.; Belfield, K. D.; Bondar, M. V.; Przhonska, O. V.; Yao, S. One- and Two-Photon Photochemical Stability of Linear and Branched Fluorene Derivatives. *J. Photochem. Photobiol., A* **2006**, *184* (1−2), 105−112.
(45) Sheik-Bahae, M.; Said, A. A.; Wei, T. H.; Hagan, D. J.; Van Stryland, E. W. Sensitive Measurement of Optical Nonlinearities Using a Single Beam. *IEEE J. Quantum Electron.* **1990**, *26* (4), 760−769.
(46) Frisch, M. J.; Trucks, G. W.; Schlegel, H. B.; Scuseria, G. E.; Robb, M. A.; Cheeseman, J. R.; Scalmani, G.; Barone, V.; Mennucci, B.; Petersson, G. A.; et al. *Gaussian 09, Revision A.2*; Gaussian, Inc.: Wallingford CT, 2009.
(47) Tomasi, J.; Mennucci, B.; Cammi, R. Quantum Mechanical Continuum Solvation Models. *Chem. Rev.* **2005**, *105* (8), 2999−3093.
(48) Masunov, A.; Tretiak, S.; Hong, J. W.; Liu, B.; Bazan, G. C. Theoretical Study of the Effects of Solvent Environment on Photophysical Properties and Electronic Structure of Paracyclophane Chromophores. *J. Chem. Phys.* **2005**, *122* (22), 224505−10.
(49) De Boni, L.; Toro, C.; Masunov, A. E.; Hernandez, F. E. Untangling the Excited States of Dr1 in Solution: An Experimental and Theoretical Study. *J. Phys. Chem. A* **2008**, *112* (17), 3886−3890.
(50) Belfield, K. D.; Bondar, M. V.; Hernandez, F. E.; Masunov, A. E.; Mikhailov, I. A.; Morales, A. R.; Przhonska, O. V.; Yao, S. Two-Photon Absorption Properties of New Fluorene-Based Singlet Oxygen Photosensitizers. *J. Phys. Chem. C* **2009**, *113* (11), 4706−4711.
(51) Mikhailov, I. A.; Bondar, M. V.; Belfield, K. D.; Masunov, A. E. Electronic Properties of a New Two-Photon Absorbing Fluorene Derivative: The Role of Hartree-Fock Exchange in the Density Functional Theory Design of Improved Nonlinear Chromophores. *J. Phys. Chem. C* **2009**, *113* (48), 20719−20724.
(52) Belfield, K. D.; Bondar, M. V.; Frazer, A.; Morales, A. R.; Kachkovsky, O. D.; Mikhailov, I. A.; Masunov, A. E.; Przhonska, O. V. Fluorene-Based Metal-Ion Sensing Probe with High Sensitivity to Zn^{2+} and Efficient Two-Photon Absorption. *J. Phys. Chem. B* **2010**, *114* (28), 9313−9321.
(53) Orr, B. J.; Ward, J. F. Perturbation Theory of Non-Linear Optical Polarization of an Isolated System. *Mol. Phys.* **1971**, *20* (3), 513−526.
(54) Kobko, N.; Masunov, A.; Tretiak, S. Calculations of the Third-Order Nonlinear Optical Responses in Push-Pull Chromophores with a Time-Dependent Density Functional Theory. *Chem. Phys. Lett.* **2004**, *392* (4−6), 444−451.
(55) Kauffman, J. F.; Turner, J. M.; Alabugin, I. V.; Breiner, B.; Kovalenko, S. V.; Badaeva, E. A.; Masunov, A.; Tretiak, S. Two-Photon Excitation of Substituted Enediynes. *J. Phys. Chem. A* **2006**, *110* (1), 241−251.
(56) Wang, S.; Hall, L.; Diev, V. V.; Haiges, R.; Wei, G.; Xiao, X.; Djurovich, P. I.; Forrest, S. R.; Thompson, M. E. N,N-Diarylanilinosquaraines and Their Application to Organic Photovoltaics. *Chem. Mater.* **2011**, *23*, 4789−4798.
(57) Shi, Y.; Lou, A. J.-T.; He, G. S.; Baev, A.; Swihart, M. T.; Prasad, P. N.; Marks, T. J. Cooperative Coupling of Cyanine and Tictoid Twisted π-Systems to Amplify Organic Chromophore Cubic Nonlinearities. *J. Am. Chem. Soc.* **2015**, *137*, 4622−4625.
(58) Varnavski, O.; Raymond, J. E.; Yoon, Z. S.; Yotsutuji, T.; Ogawa, K.; Kobuke, Y.; Goodson, T. III., Compact Self-Assembled Porphyrin Macrocycle: Synthesis, Cooperative Enhancement, and Ultrafast Response. *J. Phys. Chem. C* **2014**, *118*, 28474−28481.
(59) Salice, P.; Arnbjerg, J.; Pedersen, B. W.; Toftegaard, R.; Beverina, L.; Pagani, G. A.; Ogilby, P. R. Photophysics of Squaraine Dyes: Role of Charge-Transfer in Singlet Oxygen Production and Removal. *J. Phys. Chem. A* **2010**, *114*, 2518−2525.
(60) Feofilov, P. P.; Faerman, I. G. Absorption and Luminescence Spectra of Triphenylmethane Dyes. *Dokl. Akad. Nauk SSSR* **1952**, *87*, 931−934.
(61) Iordanov, T. D.; Davis, J. L.; Masunov, A. E.; Levenson, A.; Przhonska, O. V.; Kachkovski, A. D. Symmetry Breaking in Cationic Polymethine Dyes, Part 1: Ground State Potential Energy Surfaces and Solvent Effects on Electronic Spectra of Streptocyanines. *Int. J. Quantum Chem.* **2009**, *109* (15), 3592−3601.
(62) Gerasov, A. O.; Nayyar, I. H.; Masunov, A. E.; Przhonska, O. V.; Kachkovsky, O. D.; Melnyk, D. O.; Ryabitsky, O. B.; Viniychuk, O. O. Solitonic Waves in Polyene Dications and Principles of Charge Carrier Localization in Pi-Conjugated Organic Materials. *Int. J. Quantum Chem.* **2012**, *112* (14), 2659−2667.
(63) Masunov, A. E.; Anderson, D.; Freidzon, A. Y.; Bagaturyants, A. A. Symmetry-Breaking in Cationic Polymethine Dyes: Part 2. Shape of Electronic Absorption Bands Explained by the Thermal Fluctuations of the Solvent Reaction Field. *J. Phys. Chem. A* **2015**, *119* (26), 6807−6815.
(64) Yan, L.; Chen, X.; He, Q.; Wang, Y.; Wang, X.; Guo, Q.; Bai, F.; Xia, A.; et al. Localized Emitting State and Energy Transfer Properties of Quadrupolar Chromophores and (Multi)Branched Derivatives. *J. Phys. Chem. A* **2012**, *116*, 8693−8705.
(65) Terpetschnig, E.; Szmacinski, H.; Ozinskas, A.; Lakowicz, J. R. Synthesis of Squaraine-N-Hydroxysuccinimide Esters and Their Biological Application as Long-Wavelength Fluorescent Labels. *Anal. Biochem.* **1994**, *217*, 197−204.
(66) Yan, Z.; Xu, H.; Guang, S.; Zhao, X.; Fan, W.; Liu, X. Y. A Convenient Organic−Inorganic Hybrid Approach toward Highly Stable Squaraine Dyes with Reduced H-Aggregation. *Adv. Funct. Mater.* **2012**, *22*, 345−352.
(67) Azim, S. A.; Al-Hazmy, S. M.; Ebeid, E. M.; El-Daly, S. A. A New Coumarin Laser Dye 3-(Benzothiazol-2-Yl)-7-Hydroxycoumarin. *Opt. Laser Technol.* **2005**, *37*, 245−249.
(68) El-Daly, S. A.; El-Azim, S. A.; Elmekawey, F. M.; Elbaradei, B. Y.; Shama, S. A.; Asiri, A. M. Photophysical Parameters, Excitation Energy Transfer, and Photoreactivity of 1,4-Bis(5-Phenyl-2-Oxazolyl)Benzene (Popop) Laser Dye. *Int. J. Photoenergy* **2012**, *2012*, 1−10.
(69) Rosenthal, I. Photochemical Stability of Rhodamine 6g in Solution. *Opt. Commun.* **1978**, *24* (2), 164−166.
(70) Zepp, R. G.; Gumz, M. M.; Miller, W. L.; Gao, H. Photoreaction of Valerophenone in Aqueous Solution. *J. Phys. Chem. A* **1998**, *102*, 5716−5723.
(71) Fu, J.; Przhonska, O. V.; Padilha, L. A.; Hagan, D. J.; Van Stryland, E. W.; Belfield, K. D.; Bondar, M. V.; Slominsky, Y. L.; Kachkovski, A. D. Two-Photon Anisotropy: Analytical Description and Molecular Modeling for Symmetrical and Asymmetrical Organic Dyes. *Chem. Phys.* **2006**, *321*, 257−268.
(72) Ma, H. L.; Zhao, Y.; Liang, W. Z. Assessment of Mode-Mixing and Herzberg-Teller Effects on Two-Photon Absorption and Resonance Hyper-Raman Spectra from a Time-Dependent Approach. *J. Chem. Phys.* **2014**, *140*, 094107−17.
(73) Makarov, N. S.; Drobizhev, M.; Wicks, G.; Makarova, E. A.; Lukyanets, E. A.; Rebane, A. Alternative Selection Rules for One- and Two-Photon Transitions in Tribenzotetraazachlorin: Quasi-Centrosymmetrical π-Conjugation Pathway of Formally Non-Centrosymmetrical Molecule. *J. Chem. Phys.* **2013**, *138*, 214314−8.
(74) Ohta, K.; Antonov, L.; Yamada, S.; Kamada, K. Theoretical Study of the Two-Photon Absorption Properties of Several Asymmetrically

DOI: 10.1021/acs.jpcc.6b02446
J. Phys. Chem. C 2016, 120, 11099−11110

Substituted Stilbenoid Molecules. *J. Chem. Phys.* **2007**, *127* (8), 084504−12.
(75) Hales, J. M.; Matichak, J.; Barlow, S.; Ohira, S.; Yesudas, K.; Brédas, J.-L.; Perry, J. W.; Marder, S. R. Design of Polymethine Dyes with Large Third-Order Optical Nonlinearities and Loss Figures of Merit. *Science* **2010**, *327*, 1485−1488.
(76) Hales, J. M.; Hagan, D. J.; Van Stryland, E. W.; Schafer, K. J.; Morales, A. R.; Belfield, K. D.; Pacher, P.; Kwon, O.; Bredas, J. L.; Zojer, E. Resonant Enhancement of Two-Photon Absorption in Substituted Fluorene Molecules. *J. Chem. Phys.* **2004**, *121*, 3152−3160.
(77) Fu, J.; Padilha, L. A.; Hagan, D. J.; Van Stryland, E. W.; Przhonska, O. V.; Bondar, M. V.; Slominsky, Y. L.; Kachkovski, A. D. Experimental and Theoretical Approaches to Understanding Two-Photon Absorption Spectra in Polymethine and Squaraine Molecules. *J. Opt. Soc. Am. B* **2007**, *24* (1), 67−76.
(78) Belfield, K. D.; Bondar, M. V.; Morales, A. R.; Frazer, A.; Mikhailov, I. A.; Przhonska, O. V. Photophysical Properties and Ultrafast Excited-State Dynamics of a New Two-Photon Absorbing Thiopyranyl Probe. *J. Phys. Chem. C* **2013**, *117*, 11941−11952.
(79) Lepkowicz, R. S.; Przhonska, O. V.; Hales, J. M.; Hagan, D. J.; Van Stryland, E. W.; Bondar, M. V.; Slominsky, Y. L.; Kachkovski, A. D. Excited-State Absorption Dynamics in Polymethine Dyes Detected by Polarization-Resolved Pump-Probe Measurements. *Chem. Phys.* **2003**, *286* (2−3), 277−291.
(80) Horng, M. L.; Gardecki, J. A.; Papazyan, A.; Maroncelli, M. Subpicosecond Measurements of Polar Solvation Dynamics: Coumarin 153 Revisited. *J. Phys. Chem.* **1995**, *99*, 17311−17337.
(81) Zhang, D.; Wang, Y.; Ma, D. SiO_2 Nanoparticles as Scatterers for Random Organic Laser Action in Red fluorescent Dye 4-(Dicyanomethylene)-2-Tert-Butyl-6(1,1,7,7-Tetramethyljulolidyl-9-Enyl)-4h-Pyran Doped Polystyrene films. *J. Appl. Phys.* **2008**, *103*, 123107−4.
(82) Enciso, E.; Costela, A.; Garcia-Moreno, I.; Martin, V.; Sastre, R. Conventional Unidirectional Laser Action Enhanced by Dye Confined in Nanoparticle Scatters. *Langmuir* **2010**, *26* (9), 6154−6157.
(83) Shafer, F. P. *Dye Lasers*; Springer-Verlag: New York, 1973; p 285.

DOI: 10.1021/acs.jpcc.6b02446
J. Phys. Chem. C 2016, 120, 11099−11110